6th RIPT

LIMOGES 2013
11th to 13th December

Surface and Coatings Technology

MANUSCRIPT COVER PAGE

Title of Paper **Effect of particle size distribution of suspension feedstock on the microstructure and mechanical properties of suspension plasma spraying YSZ coatings**

Corresponding Author **:Pablo Carpio**

Full Mailing Address **:Instituto de Tecnología Cerámica (ITC). Av. Vicent Sos Baynat s/n, 12006 Castellón (Spain)**

Telephone **: 964 34 24 24**
Fax **: 964 34 24 25**
E-mail **: pablo.carpio@itc.uji.es**

Keywords **:Suspension Plasma Spraying; Yttria Stabilised Zirconia; Thermal Barrier Coating, Microstructure, Indentation**

Estimation of the length of the manuscript

(the pages of the manuscript should be numbered)

			Number of words
	Please fill out		*Please fill out*
Length of the text[1)] (using "word count")			**3498**
Number of Tables	1	**× 150**	150
Number of Figures[2)]	3	**× 150**	450
TOTAL NUMBER OF WORDS[3)] =			**4098**

[1)] Including abstract and list of references (figure captions are not included).
[2)] Each figure including Fig.a, Fig.b, Fig.c, etc. must be counted separately.
[3)] Total number of words: 4000 words for a contributed paper (oral and posters), 8000 words for an invited paper and plenary paper.
Manuscripts exceeding these word limits will not be considered for publication in the Proceedings volume. These too long papers could be submitted to the Editor of the journal for publication as regular papers.

Effect of particle size distribution of suspension feedstock on the microstructure and mechanical properties of suspension plasma spraying YSZ coatings

Pablo Carpio[1], María Dolores Salvador[2], Amparo Borrell[2], Rodrigo Moreno[3], Enrique Sánchez[1]

[1] Instituto de Tecnología Cerámica (ITC). Universitat Jaume I. Castellón, Spain

[2] Instituto de Tecnología de Materiales (ITM). Universidad Politécnica de Valencia. Valencia, Spain

[3] Instituto de Cerámica y Vidrio (ICV, CSIC), Madrid, Spain

Abstract

In this work, aqueous suspensions feedstocks with different particle size distribution from submicron and nanosized YSZ powders were prepared. A previous colloidal characterization allowed concentrated suspensions (~40 wt%) to be prepared. These suspensions were then successfully deposited by suspension plasma spraying (SPS) onto stainless steel substrates at different spraying distances. Coatings were characterised in terms of microstructure and mechanical properties (hardness and elastic modulus) by nanoindentation.

All coatings displayed a two-zones microstructure formed by partially molten areas containing nanometer or submicrometer-sized particles surrounded by fully molten areas. These partially molten areas strongly increased as standoff distance lengthened. Mechanical properties worsened with spraying distance increase. The finer the feedstock particle size the more the spraying distance effect was. A clear correlation between mechanical properties and amount of partially molten areas has been proved. Thus the use of a mixture of nano/submicronsized particles as a SPS feedstock can

represent a good balance between suspension processability and final coating performance.

Introduction

Previous research has shown that thermal barrier coatings (TBCs) obtained by suspension plasma spraying (SPS) exhibit enhanced properties when compared with conventional, APS (atmospheric plasma spraying) coatings. [1-3]. Nevertheless the properties of the resulting coatings are very dependent on the feedstock suspension properties [4,5]. Hence the first step to produce good quality SPS coatings is to suitably disperse the particles into the liquid carrier to obtain stable suspensions which can be fed into the plasma torch through the injection system without clogging or settling down [2,4]. Ethanol has been more extensively used as suspension solvent due to its lower vaporization heat but water is preferable for sustainability reasons [6]. As reported elsewhere zeta potential represents the main indicator of the dispersion degree of a given suspension [7]. Therefore, the determination of this suspension characteristic and consequently the interpretation of colloidal interactions occurring in the suspension should be the first step when a concentrated, SPS feesdsock is to be prepared. Although in principle higher solids content can be desirable in terms of deposition efficiency this content must be optimised to avoid clogging during injection as well as incomplete particle melting inside plasma torch.

With regard to particle size in the suspension feedstock SPS technology ranges from few tens of nanometers to few microns. When nanoparticles are used a much higher tendency to agglomerate is observed. Besides the particle melting in plasma torch is also deeply affected by the particle size distribution. Thus excessively small particles do

not flatten so effectively meanwhile large particles and agglomerates are more prone to remain partly unmelted [2].

Few attempts have been made to use feedstock mixtures of different particle size distributions, e.g. submicron-nano sized particles despite their many potential advantages. The use of such bimodal distribution comprising the feedstock suspension can give rise to significant benefits during the suspension processing, i.e higher solids content and lower viscosity leading to better feeding in the plasma torch along with higher deposition efficiency [4]. Besides some coatings properties can be improved when using bimodal feedstock as recently reported for APS coatings [8,9]. However, the use of these bimodal powders has not been treated in SPS literature.

Standard SPS process results in thinner coatings than those obtained by conventional APS process. As a consequence it has been successfully proved that nanoindentation technique is a more feasible method than conventional microindentation for the mechanical characterisation of such layers. However, the amount of papers dealing with the use of nanoindentation method to characterise SPS layers is still very scarce [10]. In a recent work by some of the authors [11] it was proved that hardness and elastic modulus of SPS YSZ coatings could be estimated by this technique.

In the present study, concentrated, aqueous suspension feedstocks from commercial YSZ nanoparticles and submicrometer-sized particles were prepared and stabilised so as to obtain SPS coatings at different standoff distances. A previous colloidal characterization of suspension feedstock in terms of zeta potential measurements was carried out. The coatings were microstructurally and mechanically characterised. The mechanical properties (elastic modulus and hardness) were determined by nanoindentation.

Experimental

Suspensions preparation and characterisation

A commercial YSZ nanoparticle powder (5932HT, Nanostructured and Amorphous Materials Inc., USA), and a commercial YSZ submicron-sized powder (TZ-3YS, Tosoh Co., Japan) were used as raw materials. According to the suppliers both powders contained 3 mol% ytria as well as tetragonal zirconia phase and the mean particle size was 40 nm and 400 nm for the nano and submicrometer-sized powders respectively. In addition, the nanopowder also contained some small amount of monoclinic phase (not quantified). Furthermore, a commercial salt (DURAMAX^{TM} D-3005, Rohm & Haas/Dow Chemicals, USA) of polyacrylic acid-based polyelectrolyte (PAA), with 35 wt% active matter was used as dispersing aid [12].

The colloidal stability of YSZ powders was assessed by zeta potential measurements (Zetasizer NanoZS, Malvern, UK) as a function of dispersant content and pH. In order to perform the measurements, diluted suspensions with 0.01 wt% YSZ and KCl 0.01M as electrolyte were prepared. The pH values were determined with a pH-meter (Titrino DMS 716, Metrohm, Switzerland) and were adjusted with HCl and KOH solutions. A sonication probe (UP 400S, Dr Hielscher GmbH, Germany) was used in order to avoid agglomerations which can interfere in the analysis.

Concentrated suspensions from 100% nanoparticle and 100% submicron-sized particles with a solid content of 10 vol.% could then be prepared. The optimal amount of dispersant was used and different sonication times were employed. Subsequently a bimodal (50% nanopowder/50% submicronsized powder) suspension with the same solid content was prepared following the procedure set out elsewhere [13]. The following references were used to name the suspension feedstocks: 100% nanoparticles

(Yn), 100% submicron-sized particles (Ys) and 50% nano/50% submicronsized powder (Yns).

The rheological behaviour of some concentrated suspensions was determined using a rotational rheometer (Mars, Thermo Haake Co., Thermo, Germany) operating at controlled shear rate (CR) by loading the shear rate from 0 to 1000 s^{-1} in 300 s, maintaining at 1000 s^{-1} for 60 s and uploading from 1000 to 0 s^{-1} in 300 s. The measurements were carried out at 25 ºC using a double-cone and plate system [13].

Coating deposition and characterisation

Coatings were deposited with a F4-MB monocathode torch (Sulzer Metco, Switzerland) with a 6 mm internal diameter anode operated by a robot (IRB 1400, ABB, Switzerland). The substrates were preheated between 300 ºC and 350 ºC to enhance coating adhesion. The three suspensions (Yn, Ys and Yns) were injected using a SPS system developed by the Institute for Ceramic Technology (ITC). This system is formed by two pressurised containers which force the liquid to flow through a 150 μm diameter injector. A filter was used to remove agglomerates larger than 74 μm and possible contaminations. The following spraying parameters were kept constant from previous optimisation task: 37 slpm Ar, 8 slpm H_2, 700 A intensity, 1 m/s spraying velocity and 27 ml/min suspension feed rate. Three spraying distances were tested: 30 mm, 40 mm and 50 mm.

The coatings microstructure was analyzed on polished cross-sections using a field-emission scanning electron microscope (S-4800, Hitachi, Japan). X-ray diffraction patterns were collected to identify crystalline phases in coating samples (Bruker, Theta-Theta D8 Advance, Germany). Coatings porosity as well as the amount of semi-molten areas were estimated by image analysis at 5000x magnifications from SEM pictures following a procedure set out elsewhere [13]. Limitations of this technique to estimate

very small (few hundreds of nanometers) pores were assumed [14]. Coating's hardness and elastic modulus were acquired by a G-200 nanoindenter (Agilent Technology, USA). Indentations were performed at 2000 nm constant depth using the Continuous Stiffness Measurement (CSM) method. A Berkovich diamond tip was used after the area function calibration procedure on fused silica was carried out assuring a tip radius below 100 nm. Average values of hardness and elastic modulus ware then determined for a depth range from 100 to 200 nm. More details of this procedure can be found in previous research [10, 11].

Results and discussion

Figure 1 shows the evolution of zeta potential of nano- and submicron-sized YSZ powders without dispersant and with different contents of PAA. The isoelectric point (IEP) of these powders without additives occurs at 6.2 and 6.9 respectively, in good agreement with the values reported in the literature [12]. In both cases, IEP shifted to acid pH as the PAA content increased. This demonstrates that PAA was adsorbed on particle surface leading to well dispersed suspensions at working pH. Zeta potential curve does not change significantly for PAA contents >2 wt% in the case of nanoparticle suspension and >0.5 wt% in the case of submicron-sized suspension (not shown in the figure). It means that only these amounts of PAA were adsorbed on the particles. Consequently, the calculated amount of adsorbed dispersant in both cases was 0.8 mg/m^2 which agrees with previous reported data [7]. With this information concentrated aqueous suspensions of 10 vol.% (Yn, Ys and Yns) were prepared which exhibited adequate rheological behaviour and stability so as to be injected into the plasma plume without sedimentation or clogging problems. The procedure to prepare these concentrated suspensions has been reported elsewhere [13].

Figure 2 shows the cross-sectional SEM images of the as-sprayed coatings obtained from Yn, Ys and Yns feedstocks at the three spraying distances tested (in the case of the Yn sample the longest spraying distance was not realised). As reported elsewhere all the micrographs reveal *two-zones* microstructure, named as (*I*) molten and (*II*) sintered grains areas [11, 15], which are displayed on the micrographs. For the sake of distinguishing porosity is also marked P in the micrographs. This microstructure develops because after the liquid is evaporated the resulting particles or agglomerates may thus be heated, partly melted, or melted, yielding the end coating. As a consequence the final microstructure largely depends on the characteristics of the suspension feedstock and plasma spraying conditions. As set out in the literature the heat flux significantly increases as the standoff distance diminishes giving rise to an enhanced cohesion and density in the coating [14-16]. As observed in figure 2, areas named *II* are clearly visible in all the coatings meanwhile the amount of these areas for a given feedstock seems to increase with the spraying distance. Figure 3 plots the values of the amount of partially molten areas (type *II*) and porosity determined by SEM with the spraying distance. Overall high values of type *II* areas were obtained. Furthermore the evolution of the amount of these areas with spraying distance is quite evident. As spraying distance grows the amount of partially molten areas strongly increases. These high values of unmolten areas as well as the strong variation with spraying distance can be related to the fact that highly concentrated aqueous suspensions were used. Concentrated suspension feedstock requires high mass enthalpy to melt the particles meanwhile higher staking defect density within the layer is expected. This is particularly true when water is used instead of ethanol as solvent [2,17] due to much higher enthalpy requirements of water.

Porosity data and their evolution with spraying distance are not so clear. On the one hand porosity values seem to be lower than those expected when compared with reported data obtained by other techniques [3,18]. This is probably due to the limitations associated to the assessment methodology by SEM, in particular for very small voids as mentioned earlier [14,18]. On the other hand the evolution of porosity data with spraying distance does not display an unique pattern. Hence porosity strongly increases when standoff distance rises for Yn and Ys feedstocks as expected by the evolution of the partially molten areas set out above. However, the evolution of Yns sample data does not follow this trend. This discrepancy is mainly based of an anomalous value of porosity for the 30 mm experiment probably due to the difficulty associated with the assessment of porosity in nanostructured layers. For this reason hereinafter the following discussions will be exclusively based on the amount of partially molten areas which show a much more reasonable evolution throughout the experiments carried out.

With regard to particle size of powder in the feedstock, a comparison of the amount of partially molten areas for the coatings at the three spraying distance reveals significant differences between samples. Although the effect of feedstock particle size in SPS process has been scarcely addressed, a recent review [2] points out that the particle size distribution should be rather narrow as well as the agglomeration of small particles should be also avoided. This is because excessively small particles (< 500 nm) do not effectively flatten due to their lower inertia momentum and because they may re-solidify before impacting on the substrate. In this work the agglomeration of particles in the suspension feedstocks was avoided by efficient dispersing mechanism. Thus at the shortest spraying distance Yn coating exhibits the lowest amount of partially molten areas which dramatically increases as the spraying distance rises. Ys and Yns feedstocks also display this behaviour but the variation with spraying distance is not so strong at

least from 30 mm to 40 mm spraying distance. To try to explain the differences observed between nanoparticle feedstock (Yn) and the other two feedstocks (Ys and Yns) table 1 collects viscosity values of some suspensions obtained from the three powders. Viscosity data at 1000 s^{-1} shear rate were worked out from rheological measurements as set out earlier for Yn, Ys and Yns suspensions at two solids concentration: 10 vol.% and 30 vol.%. As observed viscosity of a concentrated nanoparticle suspension is higher than that of suspensions containing submicrometer sized particles due to stronger colloidal interactions [12]. These interactions and, consequently viscosity differences between nanoparticles and submicrometer-sized particles suspensions magnifies as the solids content increases. In this way, when the suspension jet is fed into the plasma plume and the water evaporation suddenly starts to occur the viscosity of fragmented nanoparticle suspensions strongly increases making it harder for the drying of fragmented droplet to progress. For this reason water removal becomes more difficult what is particularly expectable when the plasma enthalpy starts to decrease i.e. when the standoff distance increases. This explanation agrees with the mechanism involved during the fragmentation and drying of droplets in SPS process [1,19]. Thus the melting of the outer part of the agglomerated nano/submicronsized particles injected into the plasma plume together with the sintering of the inner nano/submicronsized particles in these same agglomerates contribute to the partially molten zones development. This work highlights the role of suspension viscosity into this mechanism.

On the other hand it is worthwhile mentioning that the evolution of the amount of type *II* zones with standoff distance for Yns coating always runs below Yn sample's curve. This difference may be related to the particle packing efficiency of bimodal distribution (i.e nano/submicronsized) which results in lower viscosity values in comparison with

submicronsized distributions. This effect has already been reported in literature [20]. Thus as it can be observed in table 1 the viscosity at higher solids content of Yns suspension is slightly lower than that of Ys sample. However the complexity of the phenomena taking place during droplet formation and deposition in SPS process makes it necessary further research so as to assess the impact of suspension viscosity on the microstructure of the final deposited layers.

Finally XRD patterns of all coatings show (not provided in the paper) the presence of tetragonal phase. This is the usual phase in as-sprayed coatings when the yttria proportion is 3 mol% [11]. However small peaks of monoclinic phase were detected in those coatings obtained from feedstocks containing nanoparticles due to the presence of monoclinic phase in the nanopowder as set out above.

Figure 3 shows the variations of the average values of hardness and elastic modulus obtained for each coating versus spraying distance. Firstly the magnitude of the obtained values agrees with previous reported data [11]. Overall for each of the coatings both mechanical properties decrease when spraying distance increases. This variation clearly follows the inverse tendency undergone by the amount of type *II* zones in the coatings as can be deduced on comparing the corresponding plots in figure 3. As previously set out by the authors in YSZ SPS coatings [11] strong differences in mechanical properties were observed in the different microstructural zones (type *I* or type *II*) comprising the coatings. Unmolten or partially molten zones that are made up of partially sintered nanoparticles give rise to poor interparticle bonding. On contrary, molten particles lead to stronger cohesion in the arrangement of nanoparticles improving the mechanical properties Thus the presence of unmolten powders or partially molten particulates is desired to be minimised. Secondly with regard to the effect of the feedstock particle sizes there is not a unique trend. At the shortest spraying

distance Yn feedstock gives rise to better mechanical properties which drastically worsen when increasing the spraying distance. Bearing in mind that particle or agglomerate size in SPS feedstock can be an order of magnitude smaller or more than that in APS, it can be understood that such as small agglomerates respond very rapidly to changes in plasma temperature and velocity [17]. This behaviour can be deduced on comparing the strong variation in mechanical properties for Yn feedstock with spraying distance with a much more gradual variation for Ys powder. Finally as expected intermediate mechanical properties values can be observed for the Yns feedstock. And more importantly the feedstock comprising nano-submicronsized particles undergoes a more robust evolution of mechanical properties against heat flux changes of plasma in this case provided by changes in spraying distance.

Conclusions

YSZ aqueous, concentrated suspensions from commercial nanoparticles and submicrometer-sized particles were successfully deposited by SPS at different standoff distances. Microstructure features by SEM and mechanical properties by nanoindentation were determined in all the coatings.

Stable (without sedimentation or aging) 10 vol.% suspensions of nanoparticles, submicron-sized particles and a mixture of nano-submicrometer particles were prepared by using and adequate amount of dispersant which had been previously optimised by determining Z-potential curves. These three suspensions were used as feedstocks.

All coatings displayed a *two-zone* microstructure with fully molten areas and sintered-grains areas where the nano or sunmicrometer-structure was observed. Porosity and particularly partially-molten areas significantly increased with spraying distance due to the reduction of heat flux. Except for the shortest spraying distance, at constant spraying

distance partially molten areas strongly grew as the particle size content in the feedstock decreased (nanoparticle versus submicronsized) due probably to the impact of suspension viscosity in droplet drying.

Mechanical properties decreased as the spraying distance lengthened showing the inverse trend undergone by the amount of partially molten areas. Besides the coarser the particle size in the feedstock the more robust the variation of mechanical properties with standoff distance. In this way at intermediate or long spraying distances the coating obtained from the feedstock comprising nano and submicron-sized particles displayed the best mechanical properties values

Thus the use of a mixture of nano/submicronsized particles as a SPS feedstock can represent a good balance between suspension processability and final coating performance.

Acknowledgments

This work has been supported by the Spanish Ministry of Science and Innovation (project MAT2012-38364-C03) and co-funded by ERDF (European Regional Development Funds) and Research Promotion Plan of the Universitat Jaume I, action 2.1 (ref. E-2011-05) and action 3.1 (ref. PREDOC/2009/10).

References

1. L. Pawlowski, Surf. Coat. Technol. 203 (2009) 2807-2829.
2. P. Fauchais, G. Montavon, R.S. Lima, B.R. Marple, J. Phys. D: Appl. Phys. 44[9] (2011) 093001.
3. H. Kassner, R. Siegert, D. Hathiramani, R. Vassen, D. Stoever. J. Therm. Spray Technol. 17 (2008) 115-123.

4. D. Waldbillig, O. Kesler, Surf. Coat. Technol. 203 (2009) 2098-2101.
5. K. VanEvery, M.J.M. Krane, R.W. Trice, Surf. Coat. Technol. 206 (2012) 2464-2473.
6. A. Moign, A. Vardelle, N.J. Themelis, J.G. Legoux, Surf. Coat. Technol. 205 (2010) 668-673.
7. M. Vicent, E. Sánchez, I. Santacruz, R. Moreno, J. Eur. Ceram. Soc. 31 (2011) 1413-1419.
8. M. Vicent, E. Bannier, R. Moreno, M.D. Salvador, E. Sánchez, J. Eur. Ceram. Soc. 33 (2013) 3313-3324.
9. M.C. Bordes, M. Vicent, A. Moreno, R. Moreno, A. Borrell, M.D. Salvador, E. Sánchez, Surf. Coat. Technol. 220 (2013) 179-86.
10. E. Rayón, V. Bonache, M.D. Salvador, E. Bannier, E. Sánchez, A. Denoirjean, H. Ageorges, Surf. Coat. Technol. 206[10] (2012) 2655-2660.
11. P. Carpio, E. Rayón, L. Pawlowski, A. Cattini, R. Benavente, E. Bannier, M. D. Salvador MD, E. Sánchez, Surf. Coat. Technol. 220 (2013) 237-243.
12. R. Benavente, M.D. Salvador, M.C. Alcazar, R. Moreno, Ceram. Int. 38 (2010) 2111-2117.
13. M. Vicent, E. Bannier, R. Moreno, M.D Salvador, E. Sánchez, J. Eur. Ceram. Soc. 33 (2013) 3313-3324.
14. P. Fauchais, G. Montavon, J. Therm. Spray Technol. 19(1-2) (2010) 227-239.
15. S. Kozerski, L. Łatka, L. Pawlowski, F. Cernuschi, F. Petit, C. Pierlot, H. Podlesak, J. P. Laval, J. Eur. Ceram. Soc. 31(2011) 2089-2098.
16. C. Delbos, J. Fazilleau, V. Rat, J. F. Coudert, P. Fauchais, B. Pateyron, Plasma Chem. Plasma Process 26 (2006) 393-414.

17. O. Tingaud, P. Bertrand, G. Bertrand, Surf Coat Technol. 205 (2010) 1004-1008.
18. A. Bacciochini, G. Montavon, J. Iiavsky, A. Denoirjean, P. Fuchais, J. Therm. Spray Technol. 19[1-2] (2010) 198-206.
19. P. Fauchais, R. Etchart-Salas, V. Rat, J. F. Coudert, N. Caron, K. Wittmann-Ténèze, J. Therm. Spray Technol. 17[1] (2008) 31-59.
20. M. Vicent, E. Sánchez, T. Molina, M.I. Nieto, R. Moreno, Ceram. Int. 39 (2013) 9091-9097.

Tables

Table I. Viscosity at 1000 s^{-1} shear rate of Yn, Ys and Yns samples at two different solids content: 10 vol.% and 30 vol.%

	Viscosity (mPa·s)	
	10 vol.%	30 vol.%
Yn	2,8	46,5
Ys	1,8	17,9
Yns	2,0	13,3

Figure captions

Figure 1. Evolution of zeta potential of nano- and submicron-sized YSZ powders without dispersant and with different contents of PAA

Figure 2. Cross-sectional FEG-SEM images of the as-sprayed coatings obtained from Yn, Ys and Yns feedstocks at the three spraying distances tested (only two for Yn feedstock)

Figure 3. Evolution of partially molten areas (*type II*), porosity, hardness and elastic modulus of the coatings with spraying distance.

Figures

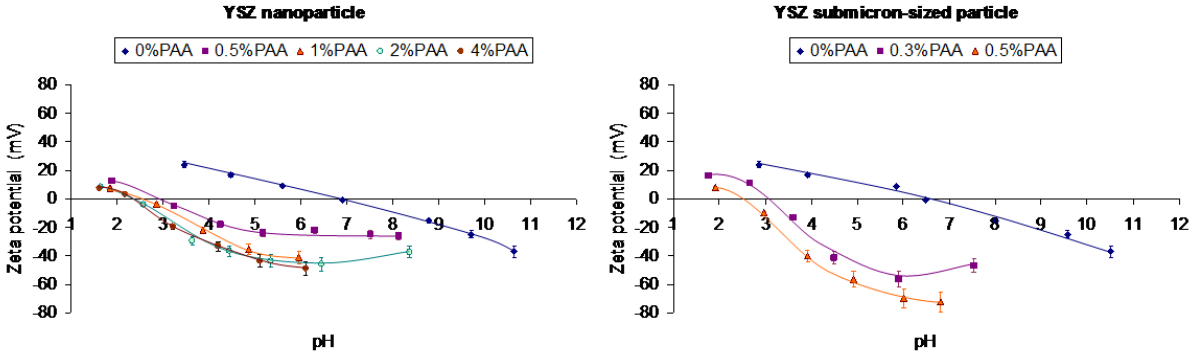
YSZ nanoparticle
0%PAA
0.5%PAA
1%PAA
2%PAA
4%PAA
Zeta potential (mV)
pH
YSZ submicron-sized particle
0%PAA
0.3%PAA
0.5%PAA
Zeta potential (mV)
pH

Figure 1

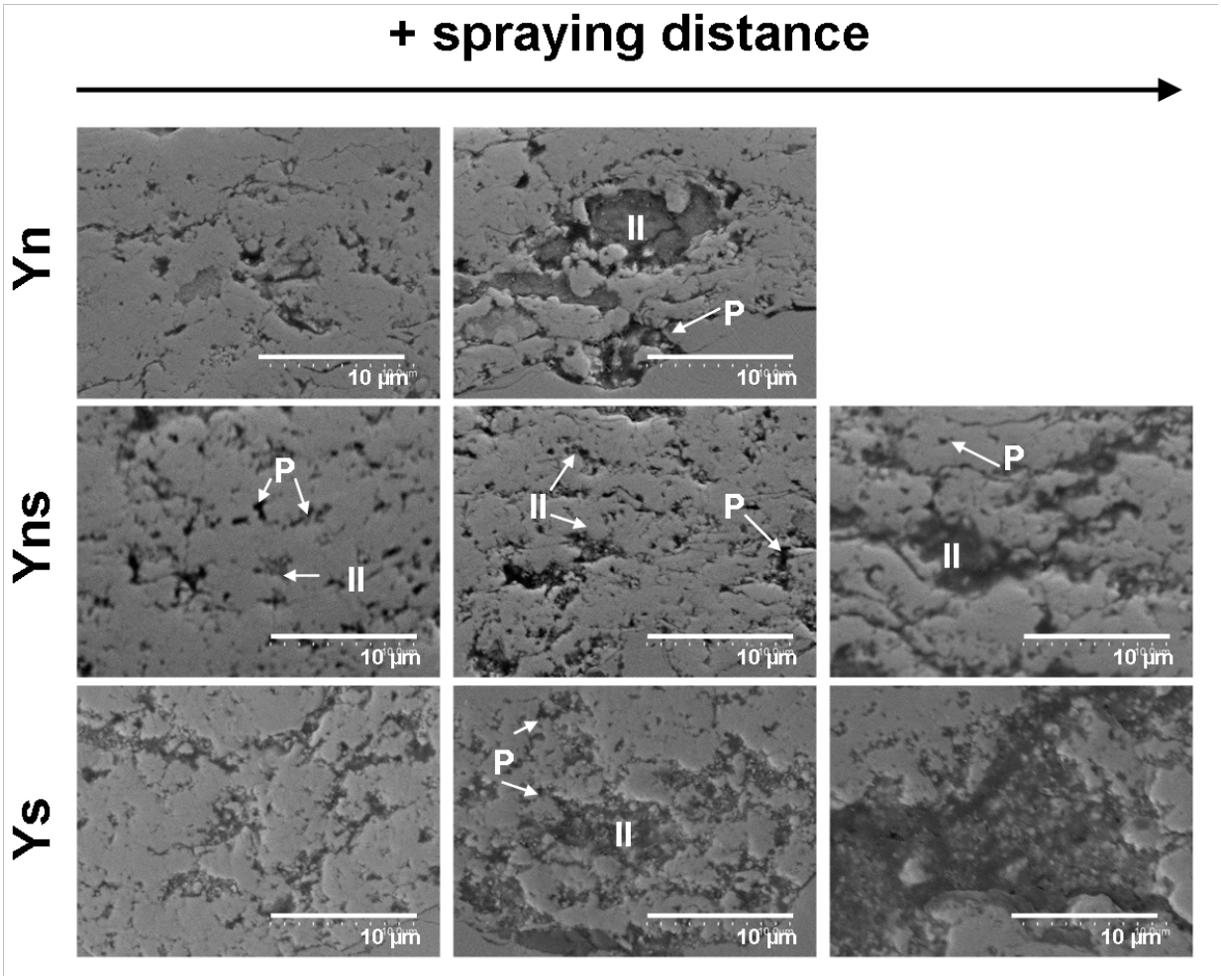

Figure 2

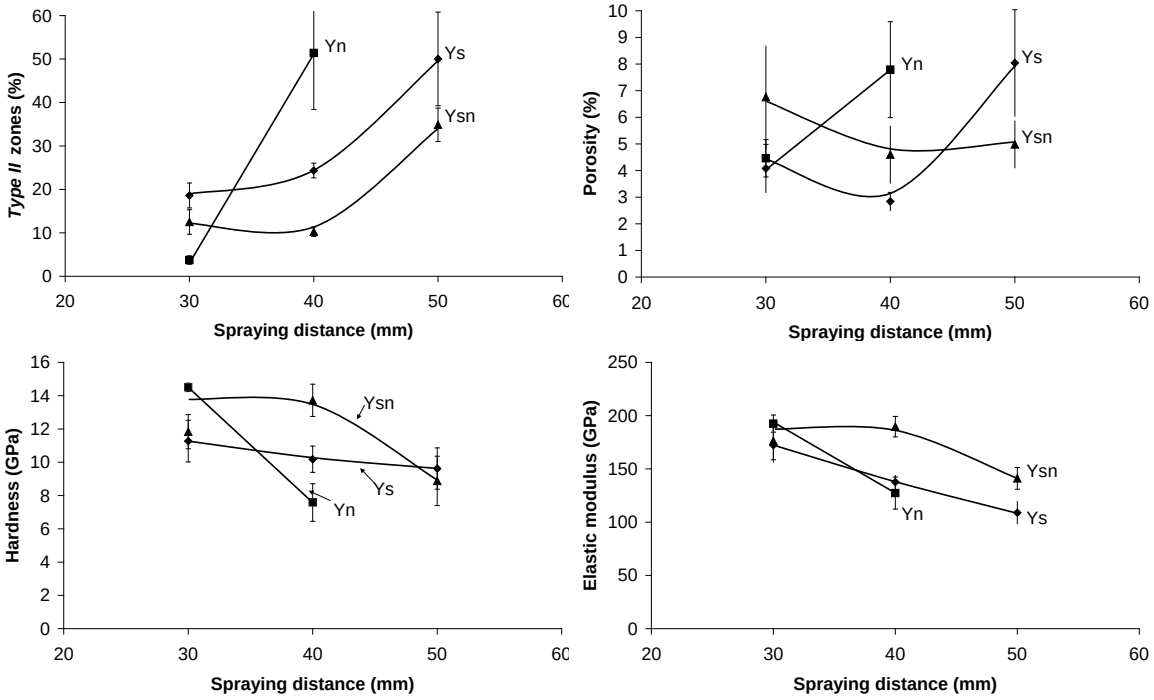
Type II zones (%)
Yn
Ys
Ysn
Spraying distance (mm)
Porosity (%)
Yn
Ys
Ysn
Spraying distance (mm)
Hardness (GPa)
Ysn
Ys
Yn
Spraying distance (mm)
Elastic modulus (GPa)
Ysn
Yn
Ys
Spraying distance (mm)

Figure 3